DIRECT ROTOR FLUX-ORIENTED CONTROL OF INDUCTION MOTORS USING HYSTERESIS CURRENT CONTROLLERS AND VSI INVERTER

OLIMPIU STOICUTA[1], VALI – CHIVUTA SIRB[2], NADIA ELENA STOICUTA[3]

Abstract: This article details the modeling and simulation of a direct rotor flux-oriented vector control system, incorporating hysteresis current controllers and a voltage source inverter (VSI). The simulations is conducted using Matlab-Simulink. The numerical analysis investigates the effects of sampling time on the discretization of speed, rotor flux, and electromagnetic torque controllers, as well as on the rotor flux observer.

Key words: rotor flux-oriented control, induction machines, simulation.

1. INTRODUCTION

Direct Rotor Flux-Oriented Control (DRFOC) is an advanced and effective technique for optimizing the performance of induction motors, widely used in industrial applications.

This method allows for the decoupling and independent control of the rotor flux and electromagnetic torque of the induction motor, similar to DC motors, thus facilitating precise and rapid control of these variables [1], [4], [5], [11].

The integration of hysteresis current controllers and a voltage source inverter (VSI) within the DRFOC system brings significant benefits in terms of stability and dynamic response of the induction motor [2].

Considering these aforementioned advantages, this article aims to elucidate, through numerical simulation in Matlab-Simulink, the impact of sampling time and discretization methods used in the controllers and the rotor flux observer on the dynamic performance of the DRFOC system, thus providing valuable insights for the improvement and optimization of industrial applications of induction motors.

[1] *Ph.D., Assoc. Prof. Eng., University of Petroşani, stoicuta_olimpiu@yahoo.com*
[2] *Ph.D., Lecturer Eng., University of Petroșani,, sirb_vali@yahoo.com*
[3] *Ph.D., Lecturer Eng. Mat., University of Petroșani,, stoicuta_nadia@yahoo.com*

2. THE VECTORIAL CONTROL SYSTEM

The vector control system discussed in this article is a direct rotor flux-oriented system, which includes hysteresis current regulators and a voltage source inverter (VSI). The block diagram of the vector control system is presented in Figure 1.

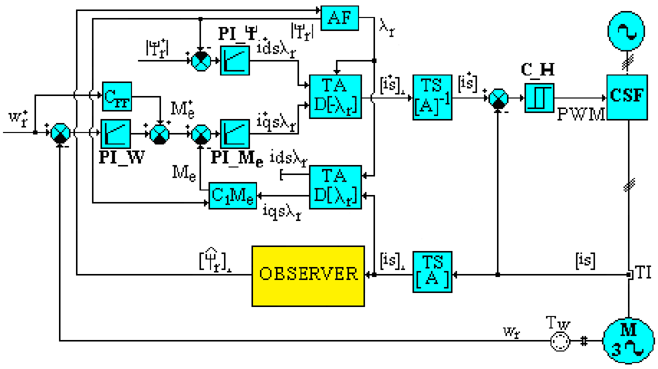

Fig.1. The vectorial control system

In Fig.1 the following notations were used: **CSF** - is the frequency static converter; **M** - is induction motor; **PI-W**, **PI_M$_e$**, **PI_Ψ** – are speed, torque and rotor flux automatic controllers; **C_H** – are hysteresis current controllers; **C$_{FF}$** - is the feedforward component of the 2DOF speed controller; **AF** - is the flux analyzer; **C$_1$M$_e$** - is torque calculation block; **TI** - are current transducers; **Tw** - is speed transducer; **TS** - is the direct and inverse Clarke transformation; **TA** - is the direct and inverse Park transformation [8], [9].

The main blocks in Fig. 1 are defined by the following mathematical models:

- ***The induction motor model (M)***. This model is defined by the following mathematical relations:

$$\frac{d}{dt}\begin{bmatrix} i_{ds} \\ i_{qs} \\ \psi_{dr} \\ \psi_{qr} \end{bmatrix} = \begin{bmatrix} a_{11} & 0 & a_{13} & a_{14}\cdot z_p\cdot\omega_r \\ 0 & a_{11} & -a_{14}\cdot z_p\cdot\omega_r & a_{13} \\ a_{31} & 0 & a_{33} & -z_p\cdot\omega_r \\ 0 & a_{31} & z_p\cdot\omega_r & a_{33} \end{bmatrix}\cdot\begin{bmatrix} i_{ds} \\ i_{qs} \\ \psi_{dr} \\ \psi_{qr} \end{bmatrix} + \begin{bmatrix} b_{11} & 0 \\ 0 & b_{11} \\ 0 & 0 \\ 0 & 0 \end{bmatrix}\cdot\begin{bmatrix} u_{ds} \\ u_{qs} \end{bmatrix} \tag{1}$$

$$J\cdot\frac{d\omega_r}{dt} = T_M - T_F - F\cdot\omega_r - T_L \tag{2}$$

where:

$$A = \begin{bmatrix} a_{11} & 0 & a_{13} & a_{14}\cdot z_p\cdot\omega_r \\ 0 & a_{11} & -a_{14}\cdot z_p\cdot\omega_r & a_{13} \\ a_{31} & 0 & a_{33} & -z_p\cdot\omega_r \\ 0 & a_{31} & z_p\cdot\omega_r & a_{33} \end{bmatrix};\ B = \begin{bmatrix} b_{11} & 0 \\ 0 & b_{11} \\ 0 & 0 \\ 0 & 0 \end{bmatrix};\ T_M = K_T\cdot\left(\psi_{dr}\cdot i_{qs} - \psi_{qr}\cdot i_{ds}\right)$$

$$a_{11}=-\left(\frac{1}{T_s\cdot\sigma}+\frac{1-\sigma}{T_r\cdot\sigma}\right);\ a_{13}=\frac{L_m}{L_s\cdot L_r\cdot T_r\cdot\sigma};\ a_{14}=\frac{L_m}{L_s\cdot L_r\cdot\sigma};\ a_{31}=\frac{L_m}{T_r};\ a_{33}=-\frac{1}{T_r};$$

$$b_{11}=\frac{1}{L_s\cdot\sigma};T_s=\frac{L_s}{R_s};T_r=\frac{L_r}{R_r};\sigma=1-\frac{L_m^2}{L_s\cdot L_r};K_T=\frac{3}{2}\cdot z_p\cdot\frac{L_m}{L_r}.$$

In previous relationships, the following notations were used: R_s, R_r – stator and rotor resistances; L_s, L_r – stator and rotor self-inductances; L_m – mutual inductance; T_s, T_r – stator and rotor time-constants; σ – leakage coefficient; z_p – number of pole pairs; J – moment of inertia of the rotor; F – friction coefficient; K_T – torque constant; T_M – instantaneous electromagnetic torque of the motor; T_F – static friction torque; F – the coefficient of viscous friction; T_L – load torque; ω_r – mechanical angular speed of the rotor; $\underline{i}_s=i_{ds}+j\cdot i_{qs}$ – space vector of the stator current; $\underline{\psi}_r=\psi_{dr}+j\cdot\psi_{qr}$ – space vector of the rotor flux; $\underline{u}_s=u_{ds}+j\cdot u_{qs}$ – space vector of the stator voltage; $j=\sqrt{-1}$.

The mathematical model of the induction motor is written in a stationary reference frame fixed to the stator (*d*-*q*).

Relations (1) and (2), after discretization using the trapezoidal robust method, become [10]:

$$\begin{bmatrix} i_{ds}\left[(k+1)\cdot T_e\right] \\ i_{qs}\left[(k+1)\cdot T_e\right] \\ \psi_{dr}\left[(k+1)\cdot T_e\right] \\ \psi_{qr}\left[(k+1)\cdot T_e\right] \end{bmatrix} = A_d\cdot\begin{bmatrix} i_{ds}\left[k\cdot T_e\right] \\ i_{qs}\left[k\cdot T_e\right] \\ \psi_{dr}\left[k\cdot T_e\right] \\ \psi_{qr}\left[k\cdot T_e\right] \end{bmatrix} + B_d\cdot\begin{bmatrix} u_{ds}\left[k\cdot T_e\right] \\ u_{qs}\left[k\cdot T_e\right] \end{bmatrix} \tag{3}$$

$$J\cdot\left\{\omega_r\left[k\cdot T_e\right]-\omega_r\left[(k-1)\cdot T_e\right]\right\}=\frac{T_e}{2}\cdot\left\{N\left[k\cdot T_e\right]+N\left[(k-1)\cdot T_e\right]\right\} \tag{4}$$

where: $$A_d=\left(I_4-A_k\cdot\frac{T_e}{2}\right)^{-1}\cdot\left(I_4+A_k\cdot\frac{T_e}{2}\right);\ B_d=\left(I_4-A_k\cdot\frac{T_e}{2}\right)^{-1}\cdot T_e\cdot B;$$

$$N(\tau)=T_M(\tau)-T_F(\tau)-F\cdot\omega_r(\tau)-T_L(\tau);$$

$$A_k=\begin{bmatrix} a_{11} & 0 & a_{13} & a_{14}\cdot z_p\cdot\omega_r\left[k\cdot T_e\right] \\ 0 & a_{11} & -a_{14}\cdot z_p\cdot\omega_r\left[k\cdot T_e\right] & a_{13} \\ a_{31} & 0 & a_{33} & -z_p\cdot\omega_r\left[k\cdot T_e\right] \\ 0 & a_{31} & z_p\cdot\omega_r\left[k\cdot T_e\right] & a_{33} \end{bmatrix}$$

In order to obtain relation (3), it was assumed that: $u_{ds}\left[k\cdot T_e\right]=u_{ds}\left[(k+1)\cdot T_e\right]$ and $u_{qs}\left[k\cdot T_e\right]=u_{qs}\left[(k+1)\cdot T_e\right]$; when the sampling time (T_e) has a very small value. The T_e denotes the sampling time used in the discretization of the mathematical model of the induction motor.

- ***The flux analyzer (AF)***. This block is defined by the following relations:

$$\begin{cases} \left|\psi_r\left[k\cdot T_n\right]\right| = \sqrt{\psi_{dr}^2\left[k\cdot T_n\right]+\psi_{qr}^2\left[k\cdot T_n\right]} \\ \sin\left(\lambda_r\left[k\cdot T_n\right]\right) = \dfrac{\psi_{qr}\left[k\cdot T_n\right]}{\left|\psi_r\left[k\cdot T_n\right]\right|};\ \cos\left(\lambda_r\left[k\cdot T_n\right]\right) = \dfrac{\psi_{dr}\left[k\cdot T_n\right]}{\left|\psi_r\left[k\cdot T_n\right]\right|} \end{cases} \tag{5}$$

- ***The torque calculation block (C_1M_e)***. The C_1M_e block is defined by the following equations:

$$M_e\left[k\cdot T_n\right] = K_a\cdot\left|\psi_r\left[k\cdot T_n\right]\right|\cdot i_{qs\lambda_r}\left[k\cdot T_n\right];\quad K_a = \frac{3}{2}\cdot z_p\cdot\frac{L_m}{L_r} \tag{6}$$

- ***The direct and inverse Clarke transformation (TS)***. These blocks are defined by the following equations:
  - *The direct Clarke transformation* (*TS [A]*)

$$\begin{cases} i_{ds}\left[k\cdot T_n\right] = i_a\left[k\cdot T_n\right] - i_{s0}\left[k\cdot T_n\right] \\ i_{qs}\left[k\cdot T_n\right] = \dfrac{1}{\sqrt{3}}\cdot\left(i_b\left[k\cdot T_n\right]-i_c\left[k\cdot T_n\right]\right) \end{cases} \tag{7}$$

where:

$$i_{s0}\left[k\cdot T_n\right] = \frac{1}{3}\cdot\left(i_a\left[k\cdot T_n\right]+i_b\left[k\cdot T_n\right]+i_c\left[k\cdot T_n\right]\right); i_c\left[k\cdot T_n\right] = -\left(i_a\left[k\cdot T_n\right]+i_b\left[k\cdot T_n\right]\right).$$

  - *The invers Clarke transformation* (*TS [A]$^{-1}$*)

$$\begin{cases} i_a^*\left[k\cdot T_n\right] = i_{ds}^*\left[k\cdot T_n\right] \\ i_b^*\left[k\cdot T_n\right] = -\dfrac{1}{2}\cdot i_{ds}^*\left[k\cdot T_n\right]+\dfrac{\sqrt{3}}{2}\cdot i_{qs}^*\left[k\cdot T_n\right] \\ i_c^*\left[k\cdot T_n\right] = -\dfrac{1}{2}\cdot i_{ds}^*\left[k\cdot T_n\right]-\dfrac{\sqrt{3}}{2}\cdot i_{qs}^*\left[k\cdot T_n\right] \end{cases} \tag{8}$$

In the previous relations, i_a, i_b and i_c are the three-phase components of the stator current (stator line currents); i_{s0} is the homopolar component of the spatial phasor of the stator current; i_a^*, i_b^* and i_c^* are the three-phase components of the command stator current.

On the other hand, i_{ds} and i_{qs} are the *d-q* components of the space vector of the stator current, and i_{ds}^*, i_{qs}^* are the *d-q* command components of the space vector of the stator current.

- ***The direct and inverse Park transformation (TA)***. These blocks are defined by the following equations:
  - *The direct Park transformation* (*TA D[λ_r]*)

$$\begin{bmatrix} i_{ds\lambda_r}\left[k\cdot T_n\right] \\ i_{qs\lambda_r}\left[k\cdot T_n\right] \end{bmatrix} = D\left[\lambda_r\left[k\cdot T_n\right]\right]\cdot\begin{bmatrix} i_{ds}\left[k\cdot T_n\right] \\ i_{qs}\left[k\cdot T_n\right] \end{bmatrix} \tag{9}$$

- *The inverse Park transformation* (*TA D[-λ_r]*)

$$\begin{bmatrix} i_{ds}^{*}\left[k\cdot T_n\right] \\ i_{qs}^{*}\left[k\cdot T_n\right] \end{bmatrix} = D\left[-\lambda_r\left[k\cdot T_n\right]\right]\cdot \begin{bmatrix} i_{ds\lambda_r}^{*}\left[k\cdot T_n\right] \\ i_{qs\lambda_r}^{*}\left[k\cdot T_n\right] \end{bmatrix} \tag{10}$$

where:

$$\left[D\left(\lambda_r\left[k\cdot T_n\right]\right)\right] = \begin{bmatrix} \cos\left(\lambda_r\left[k\cdot T_n\right]\right) & \sin\left(\lambda_r\left[k\cdot T_n\right]\right) \\ -\sin\left(\lambda_r\left[k\cdot T_n\right]\right) & \cos\left(\lambda_r\left[k\cdot T_n\right]\right) \end{bmatrix}$$

- ***The rotor flux controller* (*PI_Ψ*)**. The transfer function, in the Z-domain, of this controller is [6], [7]:

$$G_{\psi}(z) = \frac{i_{ds\lambda_r}^{*}(z)}{\varepsilon_1(z)} = K_{\psi}\cdot\left(1+\frac{1}{T_{\psi}}\cdot\frac{T_n}{2}\cdot\frac{z+1}{z-1}\right) \tag{11}$$

where $$\varepsilon_1\left[k\cdot T_n\right] = \left|\psi_r^{*}\left[k\cdot T_n\right]\right| - \left|\psi_r\left[k\cdot T_n\right]\right|$$

$$K_{\psi} = \frac{T_r}{2\cdot L_m\cdot T_{d1}^{*}};\quad T_{\psi} = T_r;\quad T_r = \frac{L_r}{R_r} \tag{12}$$

and T_{d1}^{*} is a imposed constant time.

- ***The torque controller* (*PI_M$_e$*)**. In this case, the transfer function, in the Z-domain, of this controller is [6], [7]:

$$G_M(z) = \frac{i_{qs\lambda_r}^{*}(z)}{\varepsilon_2(z)} = K_M\cdot\left(1+\frac{1}{T_M}\cdot\frac{T_n}{2}\cdot\frac{z+1}{z-1}\right) \tag{13}$$

where $$\varepsilon_2\left[k\cdot T_n\right] = M_e^{*}\left[k\cdot T_n\right] - M_e\left[k\cdot T_n\right]$$

$$K_M = \frac{T_{d1}^{*}}{K_a\cdot\left|\psi_r^{*}\right|\cdot T_{d2}^{*}};\quad T_M = T_{d1}^{*} \tag{14}$$

and T_{d2}^{*} is a imposed time constant ($T_{d2}^{*} > T_{d1}^{*}$).

- ***The speed 2DOF controller (PI_W + C$_{FF}$)***. In order to better control the speed response of the vector control system, a 2DOF speed controller is used (2DOF ~ Two-Degrees-of-Freedom Controller) [3]. The reference electromagnetic torque of the induction motor, in the case of using the Z-transform, is:

$$M_e^{*}(z) = C_{FF}(z)\cdot\omega_r^{*}(z) + M_1^{*}(z) \tag{15}$$

where $M_1^{*}(z) = G_{\omega}(z)\cdot\varepsilon_3(z)$

In relation (15), C_{FF} is the feed forward component of the 2DOF controller, and G_{ω} is a PI speed controller (PI - proportional-integral controller).

The feed forward component of the 2DOF controller is defined by the following relationship

$$G_{FF}(z)=\frac{-J\cdot\left(\frac{\omega_n}{2}\right)^2}{\frac{2}{T_n}\cdot\frac{z-1}{z+1}+\omega_n} \tag{16}$$

where: ω_n is the bandwidth of the vector control system ($\omega_n=\frac{1}{T}$, T - is the imposed time constant of the vector control system).

On the other hand, the transfer function of the PI speed controller (PI_W) is:

$$G_{\omega}(z)=\frac{M_1^*(z)}{\varepsilon_3(z)}=K_{\omega}\cdot\left(1+\frac{1}{T_{\omega}}\cdot\frac{T_n}{2}\cdot\frac{z+1}{z-1}\right) \tag{17}$$

where $\varepsilon_3[k\cdot T_n]=\omega_r^*[k\cdot T_n]-\omega_r[k\cdot T_n]$

$$K_{\omega}=\frac{T_4\cdot(1+\rho^2)}{2\cdot K_4\cdot T_{d2}^*}\ ;\quad T_{\omega}=4\cdot\frac{T_{d2}^*\cdot(1+\rho^2)}{(1+\rho)^3}\ ;\ \rho=\frac{T_{d2}^*}{T_4}\ ;\ K_4=\frac{1}{F};\ T_4=\frac{J}{F} \tag{18}$$

All the previously presented controllers have been discretized using the trapezoidal method.

- ***The hysteresis current controllers (C_H)***. In this case, the PWM (Pulse-width modulation) pulses for the VSI inverter are generated using the following relationships:

$$S_1[k\cdot T_n]=\begin{cases}0 & if \quad \varepsilon_4[k\cdot T_n]\le-\Delta_h\\ 1 & if \quad \varepsilon_4[k\cdot T_n]\ge\Delta_h\\ S_1[(k-1)\cdot T_n] & if \quad |\varepsilon_4[k\cdot T_n]|<\Delta_h\end{cases};\varepsilon_4[k\cdot T_n]=i_a^*[k\cdot T_n]-i_a[k\cdot T_n] \tag{19}$$

$$S_2[k\cdot T_n]=\begin{cases}0 & if \quad \varepsilon_5[k\cdot T_n]\le-\Delta_h\\ 1 & if \quad \varepsilon_5[k\cdot T_n]\ge\Delta_h\\ S_2[(k-1)\cdot T_n] & if \quad |\varepsilon_5[k\cdot T_n]|<\Delta_h\end{cases};\varepsilon_5[k\cdot T_n]=i_b^*[k\cdot T_n]-i_b[k\cdot T_n] \tag{20}$$

$$S_3[k\cdot T_n]=\begin{cases}0 & if \quad \varepsilon_6[k\cdot T_n]\le-\Delta_h\\ 1 & if \quad \varepsilon_6[k\cdot T_n]\ge\Delta_h\\ S_3[(k-1)\cdot T_n] & if \quad |\varepsilon_6[k\cdot T_n]|<\Delta_h\end{cases};\varepsilon_6[k\cdot T_n]=i_c^*[k\cdot T_n]-i_c[k\cdot T_n] \tag{21}$$

where Δ_h is the hysteresis band of the current controllers.

- ***The rotor flux observer***. This observer uses as inputs the rotor speed as well as the *d-q* components of the stator currents of the induction motor. This observer is defined by the following mathematical relations:

$$\frac{d}{dt}\begin{bmatrix}\hat{\psi}_{dr}\\ \hat{\psi}_{qr}\end{bmatrix}=F\cdot\begin{bmatrix}\hat{\psi}_{dr}\\ \hat{\psi}_{qr}\end{bmatrix}+H\cdot\begin{bmatrix}i_{ds}\\ i_{qs}\end{bmatrix} \tag{22}$$

where

$$F = \begin{bmatrix} -\frac{1}{T_r} & -z_p \cdot \omega_r \\ z_p \cdot \omega_r & -\frac{1}{T_r} \end{bmatrix};\ H = \begin{bmatrix} \frac{L_m}{T_r} & 0 \\ 0 & \frac{L_m}{T_r} \end{bmatrix} \tag{23}$$

The discrete model of the rotor flux observer (22) is given by the following relation

$$\begin{bmatrix} \hat{\psi}_{dr}\left[(k+1)\cdot T_n\right] \\ \hat{\psi}_{qr}\left[(k+1)\cdot T_n\right] \end{bmatrix} = F_d \cdot \begin{bmatrix} \hat{\psi}_{dr}\left[k \cdot T_n\right] \\ \hat{\psi}_{qr}\left[k \cdot T_n\right] \end{bmatrix} + H_d \cdot \begin{bmatrix} i_{ds}\left[k \cdot T_n\right] \\ i_{qs}\left[k \cdot T_n\right] \end{bmatrix} \tag{24}$$

where:

$$F_d = \sum_{i=0}^{3} \frac{F_k^i \cdot T_n^i}{i!};\ H_d = \sum_{i=0}^{2} \frac{F_k^i \cdot T_n^{i+1}}{(i+1)!} \cdot H \tag{25}$$

$$F_k = \begin{bmatrix} -\frac{1}{T_r} & -z_p \cdot \omega_r\left[k \cdot T_n\right] \\ z_p \cdot \omega_r\left[k \cdot T_n\right] & -\frac{1}{T_r} \end{bmatrix} \tag{26}$$

The previous relationships are obtained based on the ZOH (Zero Order Hold) discretization method. For the purpose of discretization, the matrices F_d and H_d are truncated (terms for which the sampling time (T_n) has an order greater than three are neglected).

In the previous relationships, T_n is the sampling time used in the discretization of the relationships that define the control algorithm for the vector control system of the induction motor.

3. THE SIMULATIONS RESULTS

In order to highlight the effects of sampling time on the dynamic performance of the vector control system, we will use a 3kW induction motor with the electrical and dynamic parameters presented in Table 1.

In numerical simulation tests, the sampling times used are:

- Case 1: $T_n = 20[\mu s];\ T_e = 1[\mu s]$;
- Case 2: $T_n = 100[\mu s];\ T_e = 1[\mu s]$.

Table 1. ***The electrical and mechanical parameters of the induction motor [2]***

	Name	Value		Name	Value
R_s	*Stator resistance*	2.0975 [Ω]	J	*Motor inertia*	0.1[kg·m^2]
R_r	*Rotor resistance*	2.0625 [Ω]	F	*Friction coefficient*	0.04[N·m·s/rad]
L_s	*Stator inductance*	0.1202 [H]	n_N	*Rated speed*	705 [rpm]

L_r	*Rotor inductance*	0.1263 [H]	z_p	*Number of pole pairs*	4
L_m	*Mutual inductance*	0.1158 [H]	f_N	*Rated frequency*	50 [Hz]
U_N	*Rated voltage*	380 [V]	M_N	*Rated torque*	40 [N·m]

In the case of both tests conducted through simulation, it is assumed that the induction motor operates in load, with a load torque equal to its rated torque. On the other hand, in the simulations the hysteresis band of the current controllers is $\Delta_h = 1/12\,[A]$ and bandwidth of the vector control system is $\omega_n = 100\,[rad/s]$. In order to tune the controllers, the following time constants were used: $T_{d1}^* = 1\,[ms]$; $T_{d1}^* = 7.5\,[ms]$.

The simulation results are presented in the following figures.

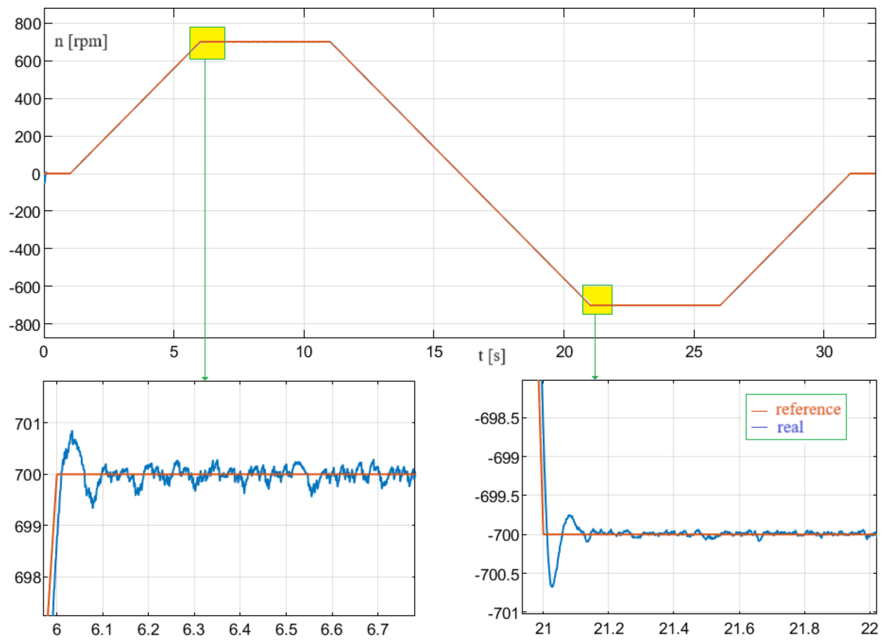

Fig.2. The time variation of the induction motor speed ~ Case 1

From Fig. 2, it can be observed that the speed of the induction motor stabilizes rapidly, indicating good dynamic performance of the vector control system when using a sampling time of 20 [μs].

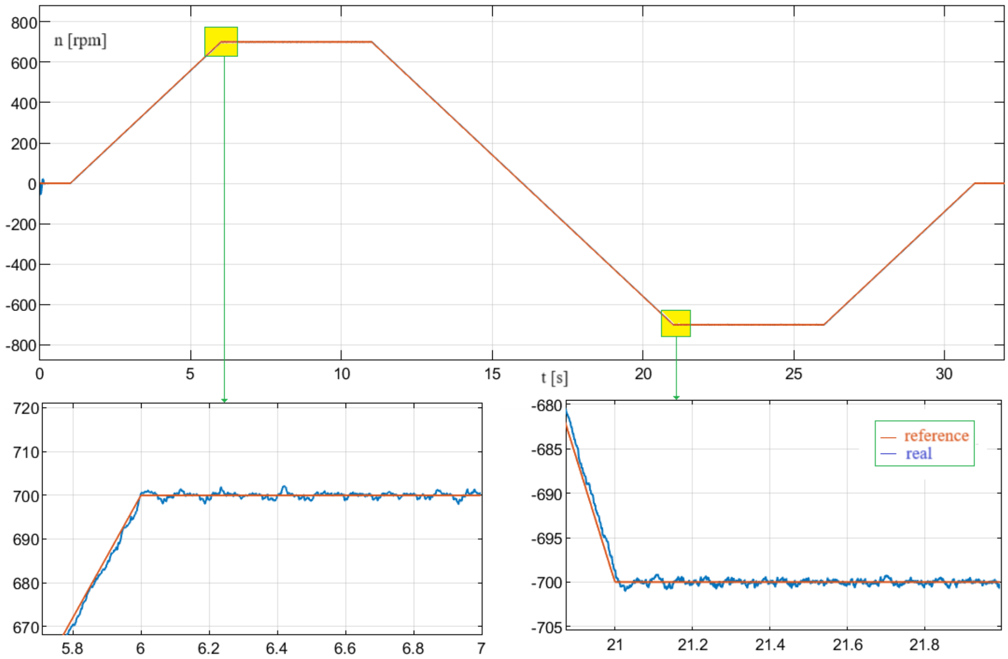

Fig.3. The time variation of the induction motor speed ~ Case 2

On the other hand, from Fig. 3, it can be observed that the speed of the induction motor exhibits larger oscillations and slower stabilization compared to Case 1, suggesting poorer dynamic performance due to the larger sampling time.

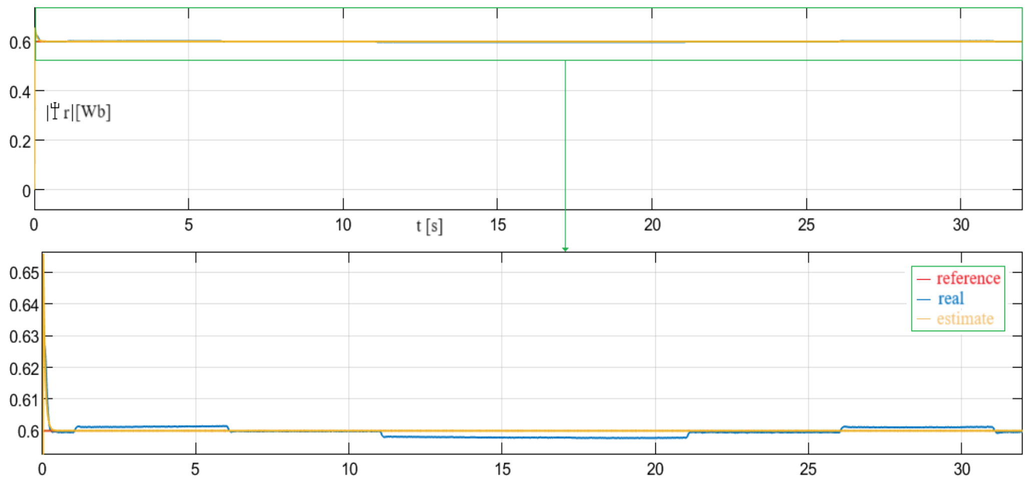

Fig.4. The rotor flux space vector - absolute value ~ Case 1

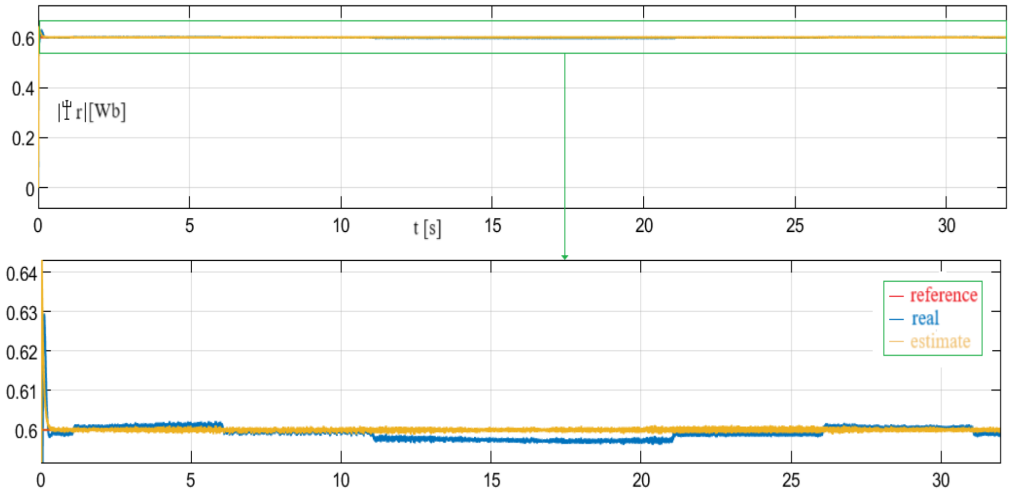

Fig.5. The rotor flux space vector - absolute value ~ Case 2

From Fig. 4 and Fig. 5, it can be observed that the absolute value of the spatial vector of the rotor flux of the induction motor is considerably more stable and constant in Case 1, compared to Case 2, where more pronounced variations and reduced stability are manifested. These observations suggest a significant negative influence of a larger sampling time on the performance of the vector control system.

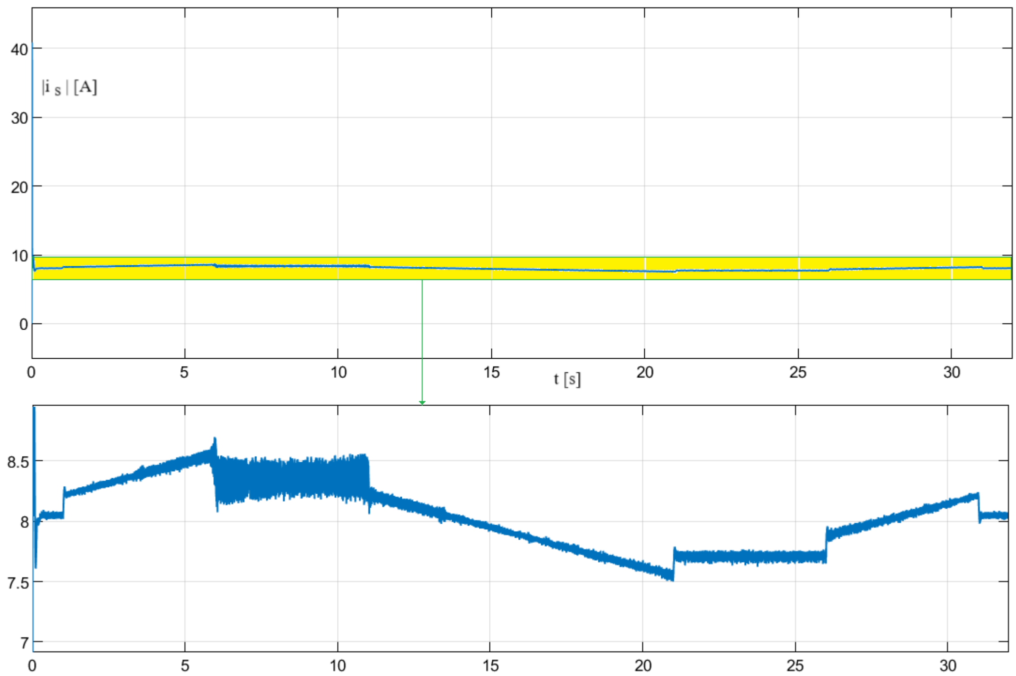

Fig.6. The stator current space vector - absolute value ~ Case 1

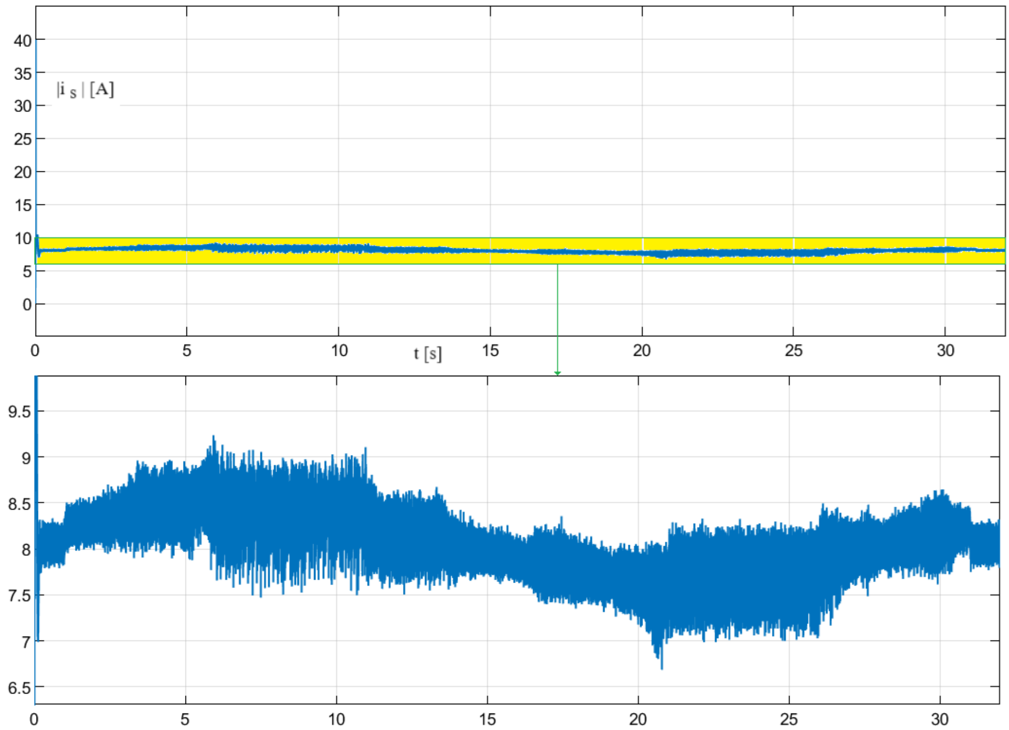

Fig.7. The stator current space vector - absolute value ~ Case 2

Analyzing Fig. 6 and Fig. 7, it is found that in Case 1, the absolute value of the spatial vector of the stator current has much smaller fluctuations and much better stability compared to Case 2.

4. CONCLUSIONS

Direct Rotor Flux Oriented Control (DRFOC) significantly improves the dynamic performance of induction motors, ensuring precise control of flux and electromagnetic torque. Simulations have shown that a smaller sampling time (20 [µs]) provides superior stability and performance compared to a larger sampling time (100 [µs]).

The detailed mathematical models presented in this article, along with the results obtained from Matlab-Simulink simulations, provide valuable support for experts in the field of induction motor control.

The research presented in this article can be extended in the future to optimize the selection of sampling time and control strategy, so that the efficiency and reliability of the induction motor control system are significantly improved. Additionally, the integration of emerging technologies, such as machine learning and artificial intelligence, can facilitate the development of advanced control and predictive maintenance methods for these motors.

REFERENCES

[1]. Boldea I., Nasar S.A., *Vector Control of AC Drives*, CRC Press, 1992.

[2]. Bitoleanu A., Popescu M., Suru V., *Experimental Evaluation of Rotor Field orientation Control and Hysteresis Controller for Induction Traction Motor*, 12th International Symposium on Advanced Topics in Electrical Engineering (ATEE), Bucharest, Romania, pp. 1-6, 2021.

[3]. Gogea A., Stoicuta O., Pana T., *Comparative Analysis Between the PI Speed Controller and Two-Degrees-of-Freedom Speed Controller for Induction Motor Drive*, 2019 8th International Conference on Modern Power Systems (MPS), Cluj-Napoca, Cluj, Romania, pp. 1-6, 2019.

[4]. Kelemen A., Imecs M., *Field-oriented AC Electrical Drives*, Romania Academy Publishing House, Bucharest, 1989.

[5]. Pana T., Stoicuta O., *Stability of the Vector Drive Systems with Induction Motors*, Mediamira Publishers, 2016.

[6]. Pana T., Stoicuta O., *Controllers tuning for the speed vector control of induction motor drive systems*, IEEE International Conference on Automation, Quality and Testing, Robotics (AQTR), Cluj-Napoca, Romania, pp. 1-6, 2010.

[7]. Stoicuta O., Pana T., *Asymptotic stability study of induction motor sensorless vector control systems with MRAS observer*, IEEE International Conference on Automation, Quality and Testing, Robotics (AQTR), Cluj-Napoca, Romania, pp. 1-6, 2016.

[8]. Stoicuta O., *The utilization of the S-Function block in simulation of the Luenberger rotor flux observer for induction motors*, Annals of the University of Petrosani, Electrical Engineering, Vol.18, pp. 31- 46, 2016.

[9]. Stoicuta O., *The utilization of the S-Function block in simulation of the mathematical model of induction motor with iron loss*, Annals of the University of Petrosani, Electrical Engineering, Vol.18, pp. 5-20, 2016.

[10]. Stoicuta O., Campian H., Pana T., *The Comparative Study of the Stability of the Vector Control Systems That Contain In the Loop Luenberger and Kalman Type Estimators*, IEEE International Conference on Automation, Quality and Testing, Robotics, Cluj-Napoca, Romania, , pp. 113-117, 2006.

[11]. Vas P., *Vector Control of AC Machines*, CRC Oxford, 1990.